The nuclear EoS: from experiments to astrophysical observations

Isaac Vidaña, INFN Catania

Istituto Nazionale di Fisica Nucleare

21st ZIMANYI SCHOOL WINTER WORKSHOP ON HEAVY ION PHYSICS, December 6th-10th 2021, Budapest, Hungary

In this talk …

I will review different experimental and astrophysical observational constraints of the nuclear EoS as well as some of the phenomenological models & ab-initio theoretical many-body approaches commonly used in its description

Two recent excellent reviews on the topic are

- Oertel, Hempel, Klahn & Typel, Rev. Mod. Phys. 89, 015007 (2017)
- Burgio & Fantina, in "The Physics & Astrophysics of Neutron Stars", Springer-Verlag 2018

What do we know to build the nuclear EoS ?

✧ Masses, radii & other properties of more than 3000 isotopes

✧ Scattering (cf. > 4000 NN data for E_{lab} < 350 MeV)

J. Erler et al., Nature 486, 509 (2012)

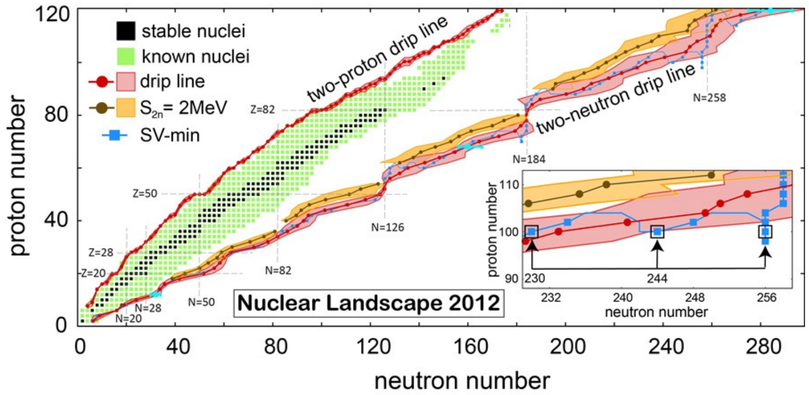

➢ Around ρ_0 & β=0 the nuclear EoS can be characterized by a few isoscalar (E_0 ,K_0, Q_0) & isovector (E_{sym}, K_{sym}, Q_{sym}) parameters which can be constrained by nuclear experiments & astrophysical observables

$$\frac{E}{A}(\rho,\beta) = E_0 + \frac{1}{2}K_0x^2 + \frac{1}{6}Q_0x^3 + \left(E_{sym} + Lx + \frac{1}{2}K_{sym}x^2 + \frac{1}{6}Q_{sym}x^3\right)\beta^2 + \cdots \quad , \quad x = \frac{\rho-\rho_0}{3\rho_0}$$

➢ Extrapolation to high densities should rely on theoretical models to be tested with astrophysical observations

Constraints from Nuclear Physics Experiments

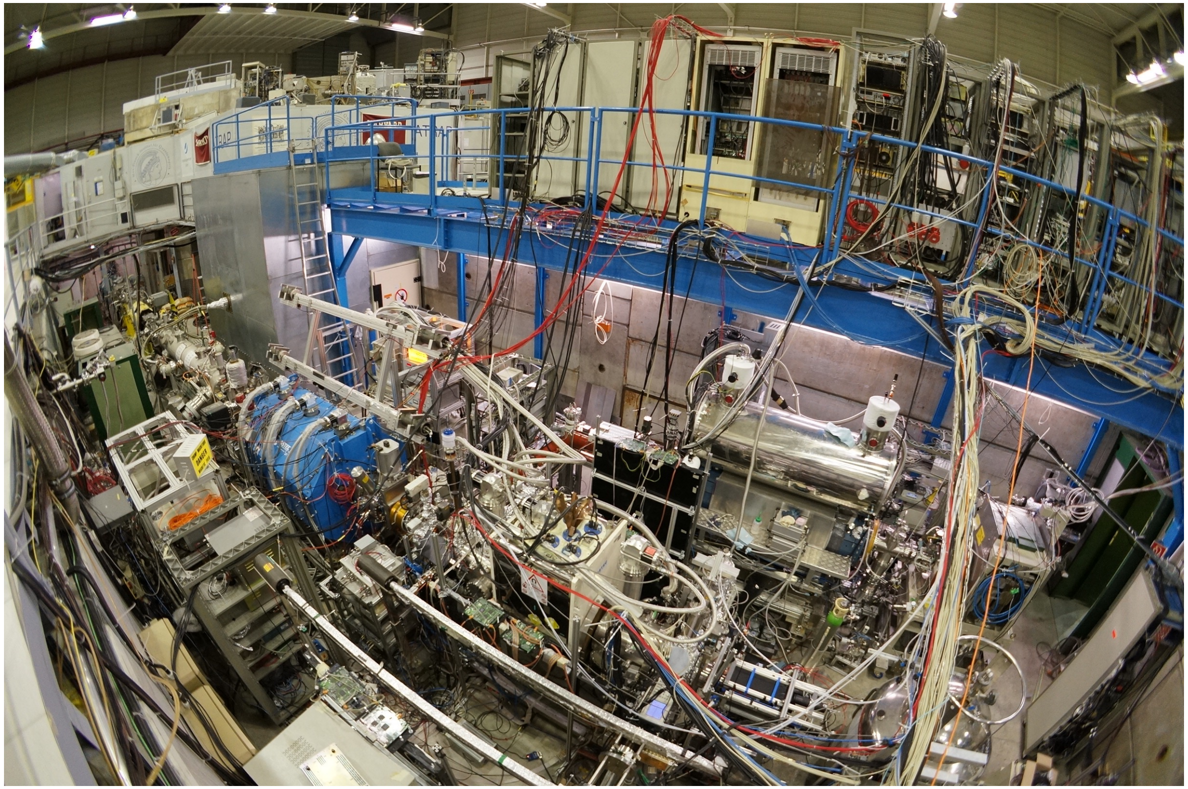

Density Distributions & Nuclear Binding Energies

✧ **Density distributions:**

(e,e') elastic scattering, hadron proves $\xrightarrow{A=N+Z\to\infty}$ $\rho_0 \sim 0.16 \ \ \text{fm}^{-3}$

✧ **Nuclear binding energies:**

$$B(N,Z) = a_v A + a_s A^{2/3} + a_c \frac{Z^2}{A^{1/3}} + \left(a_{Av} A + a_{As} A^{2/3}\right)\frac{(N-Z)^2}{A^2} + \delta a_p A^{-1/2}$$

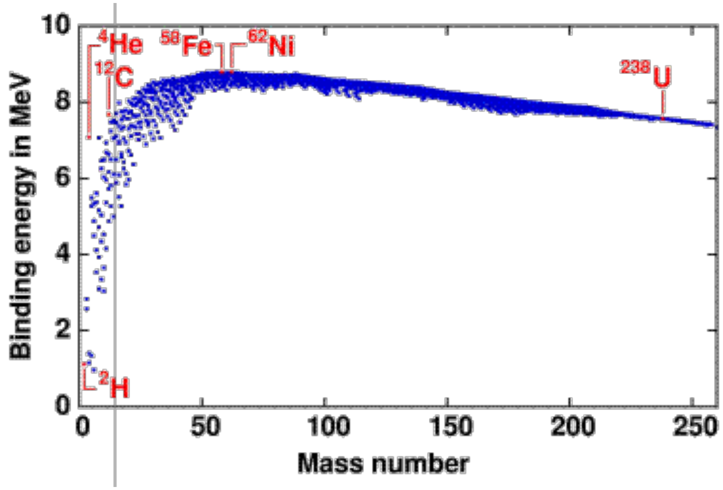

Measurements of nuclear binding energies allow the identification

$$a_V \Leftrightarrow B_{sat} = -E_0$$
$$a_{Av} \Leftrightarrow E_{sym}$$

(in the limit $A = N + Z \to \infty$)

Recent fits of binding energies with non-relativistic & relativistic EDF give

SHF models: $B_{sat} = (15.96 \pm 0.31)$ MeV, $E_{sym} = (31.2 \pm 6.7)$ MeV

RMF models: $B_{sat} = (16.13 \pm 0.51)$ MeV, $E_{sym} = (33.4 \pm 4.7)$ MeV

Dutra et al., PRC 85, 035201 (2012); PRC 90, 055203 (2014)

Nuclear Resonances

✧ ISGMR

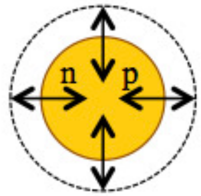

ΔL=0
ΔS=0, ΔT=0

K_0 from the measurement of excitation energy E_{ISGMR}

Typical values in the range ~ 210 – 270 MeV

Phys. Rep. 64, 171 (1980); PRC 90, 055203 (2014)

✧ IVGDR

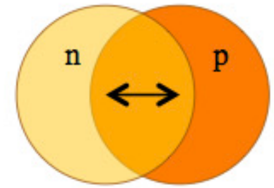

ΔL=1
ΔS=0, ΔT=1

Symmetry energy influences the excitation energies of IVGDR. Their analysis allows to determine E_{sym}

$$23.3 < E_{sym}\left(\rho = 0.1\text{fm}^{-3}\right) = 24.9 \quad \text{MeV}$$

Trippa et al., PRC 77, 061304 (R) (2008)

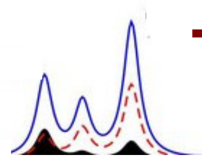

✧ ISGQR & IVGDR

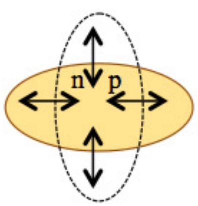

ΔL=2
ΔS=0, ΔT=0

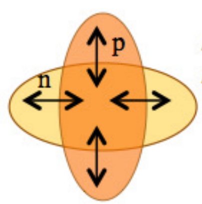

ΔL=2
ΔS=0, ΔT=1

Correlation of Δr_{np} with ISGQR & IVGQR excitation energies from which

$$\Delta\left({}^{208}\text{Pb}\right) = 0.14 \pm 0.03 \quad \text{fm}, \qquad L = 37 \pm 18 \quad \text{MeV}$$

Roca-Maza et al., PRC 87, 037301 (2013)

✧ PDR

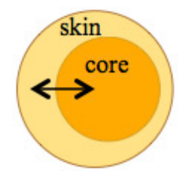

Collective oscillation of neutron skin against the core

Sensitive to the symmetry energy. A recent analysis of PDR in ^{68}Ni & ^{132}Sn using RPA models for the dipole response based in Skyrme & RMF give

$$E_{sym} = 32.3 \pm 1.3 \quad \text{MeV}, \qquad L = \quad 64.8 \pm 15.7 \quad \text{MeV}$$

Carbone et al., PRC 81, 041301 (R) (2010)

Neutron Skin Thickness & Electric Dipole Polarizability

✧ Neutron skin thickness Δr_{np}

Accurate measurements of Δr_{np} via parity-violating electron scattering or antiprotonic atom data can constrain $E_{sym}(\rho)$, particulary L via its strong correlation with Δr_{np}

PREX-II experiment PRL 126, 172502 (2021

$\Delta(^{208}Pb) = 0.283 \pm 0.071$ fm $\longrightarrow$ E_{sym} = 34-42 MeV,
L = 74-149 MeV

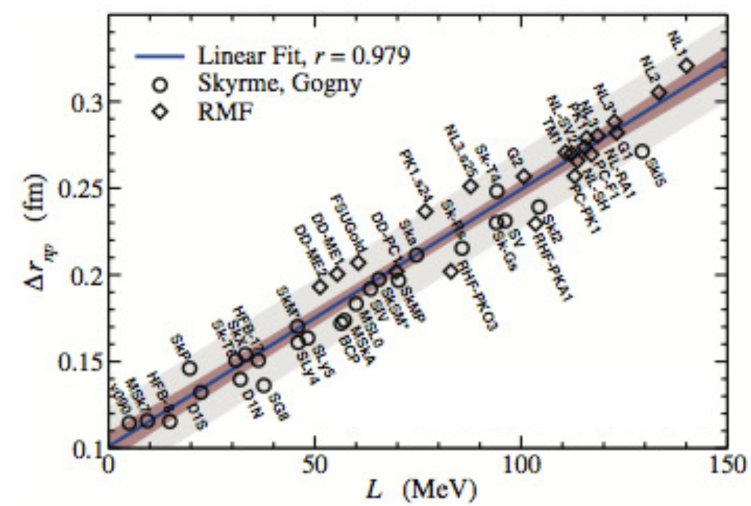

✧ Electric dipole polarizability α_D

Information on $E_{sym}(\rho)$ from available data of α_D of ^{68}Ni, ^{120}Sn & ^{208}Pb. Strong correlation of $\alpha_D E_{sym}$ with L

$$E_{sym} = 30-35 \;\; \text{MeV}, \quad L = 22-66 \;\; \text{MeV}$$

$$\Delta r_{np}(^{68}\text{Ni}) = 0.15-0.19 \;\; \text{fm}$$

$$\Delta r_{np}(^{120}\text{Sn}) = 0.12-0.16 \;\; \text{fm}$$

$$\Delta r_{np}(^{208}\text{Pb}) = 0.13-0.19 \;\; \text{fm}$$

Roca-Maza et al., PRC 92, 064304 (2015)

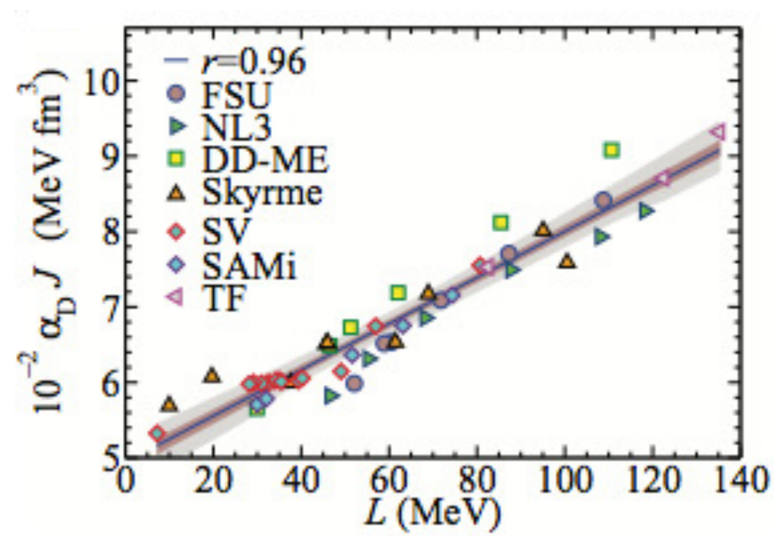

EoS from Heavy Ion Collisions

The analysis of data from HIC requires the use of transport models which do not depend directly on the EoS but rather on the mean field of the participant particles & the in-medium cross sections of the relevant reactions

However, there are several transport codes in the market. A natural question arises: How much the results depend on the transport codes ?

P. Danielewicz et al., Science 298, 1592 (2002)

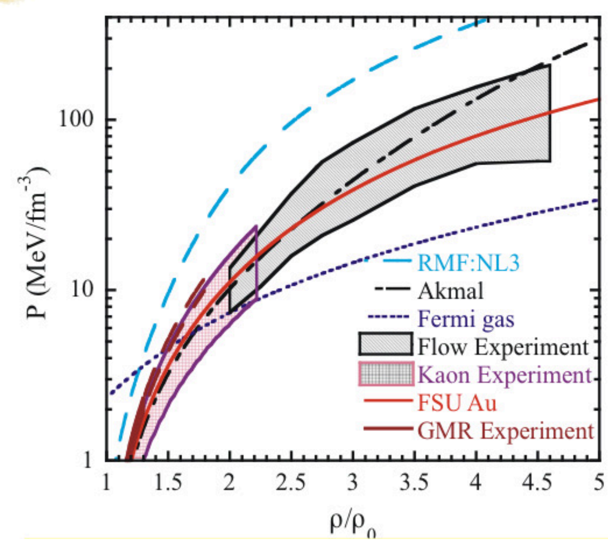

Several observables in HIC are sensitive to the nuclear EoS

sub-saturation densities

- ✓ n/p & t/^{3}He ratios
- ✓ isospin fragmentation & isospin scaling
- ✓ np correlation functions at low rel. mom.
- ✓ isospin difussion/transport
- ✓ neutron-proton differential flow

supra-saturation densities

- ✓ π^-/π^+ & K^-/K^+ ratios
- ✓ np differential transverse flow
- ✓ nucleon elliptic flow at high trans. mom.
- ✓ n/p ratio of squeezed out nucleons perpendicular to the reaction plane

Astrophysical Constraints

Neutron Star Masses

NS masses can be inferred directly from observations of binary systems

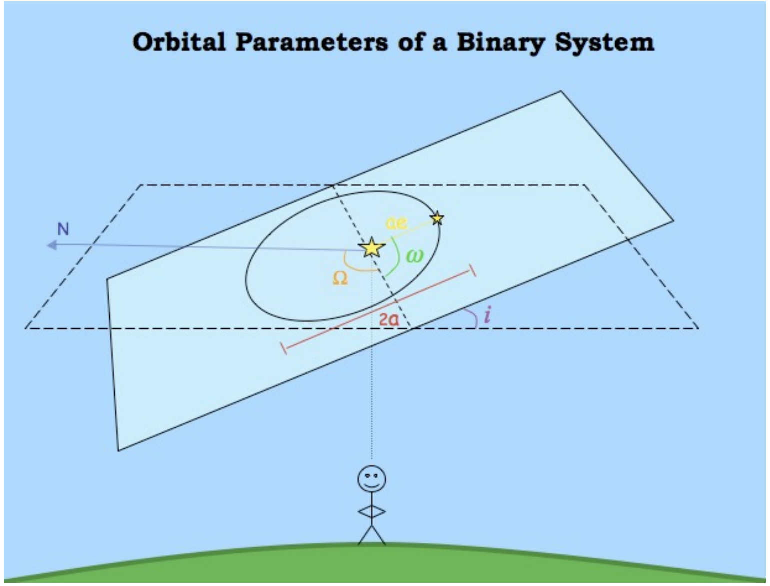

- 5 orbital (Keplerian) parameters can be precisely measured:
  - ✓ Orbital period (P)
  - ✓ Projection of semimajor axis on line of sight (a sin i)
  - ✓ Orbit eccentricity (ε)
  - ✓ Time of periastron (T_0)
  - ✓ Longitude of periastron (ω_0)
- 3 unknowns: M_1, M_2, i

Kepler's 3rd law

$$\frac{G(M_1+M_2)}{a^3}=\left(\frac{2\pi}{P}\right)^2 \rightarrow$$

$$f(M_1,M_2,i)\equiv\frac{(M_2\sin i)^3}{(M_1+M_2)^2}=\frac{Pv^3}{2\pi G}$$

mass function

In few cases small deviations from Keplerian orbit due to GR effects can be detected

Measure of at least 2 post-Keplerian parameters → High precision NS mass determination

$$\dot{\omega} = 3T_{\otimes}^{2/3}\left(\frac{P_b}{2\pi}\right)^{-5/3}\frac{1}{1-\varepsilon}\left(M_p + M_c\right)^{2/3} \longrightarrow$$ Advance of the periastron

$$\gamma = T_{\otimes}^{2/3}\left(\frac{P_b}{2\pi}\right)^{1/3}\varepsilon\frac{M_c\left(M_p + 2M_c\right)}{\left(M_p + M_c\right)^{4/3}} \longrightarrow$$ Time dilation & grav. redshift

$$r = T_{\otimes}M_c \longrightarrow$$ Shapiro delay "range"

$$s = \sin i = T_{\otimes}^{-1/3}\left(\frac{P_b}{2\pi}\right)^{-2/3}x\frac{\left(M_p + M_c\right)^{2/3}}{M_c} \longrightarrow$$ Shapiro delay "shape"

$$\dot{P}_b = -\frac{192\pi}{5}T_{\otimes}^{5/3}\left(\frac{P_b}{2\pi}\right)^{-5/3}f(\varepsilon)\frac{M_p M_c}{\left(M_p + M_c\right)^{1/3}} \longrightarrow$$ Orbit decay due to GW emission

Recent Measurements of High NS Masses

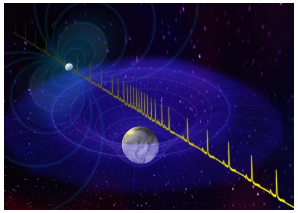

- **PSR J164-2230** (Demorest et al. 2010)

  - ✓ binary system (P=8.68 d)
  - ✓ low eccentricity ($\varepsilon=1.3 \times 10^{-6}$)
  - ✓ companion mass: $\sim 0.5 M_\odot$
  - ✓ pulsar mass: $M = 1.928 \pm 0.017 M_\odot$

In this decade NS with $2M_\odot$ have been observed by measuring Post-Keplerian parameters of their orbits

- Advance of the periastron $\dot{\omega}$
- Shapiro delay (range & shape)
- Orbital decay $\dot{P}_b$
- Grav. redshift & time dilation γ

- **PSR J0348+0432** (Antoniadis et al. 2013)

  - ✓ binary system (P=2.46 h)
  - ✓ very low eccentricity
  - ✓ companion mass: $0.172 \pm 0.003 M_\odot$
  - ✓ pulsar mass: $M = 2.01 \pm 0.04 M_\odot$

- **MSP J0740+6620** (Cromartie et al. 2020)

  - ✓ binary system (P=4.76 d)
  - ✓ low eccentricity ($\varepsilon=5.10(3) \times 10^{-6}$)
  - ✓ companion mass: $0.258(8) M_\odot$
  - ✓ pulsar mass: $M = 2.14^{+0.10}_{-0.0.9} M_\odot$ (68.3% c.i.)

    $M = 2.14^{+0.20}_{-0.018} M_\odot$ (95.4% c.i.)

Measured Neutron Star Masses (2021)

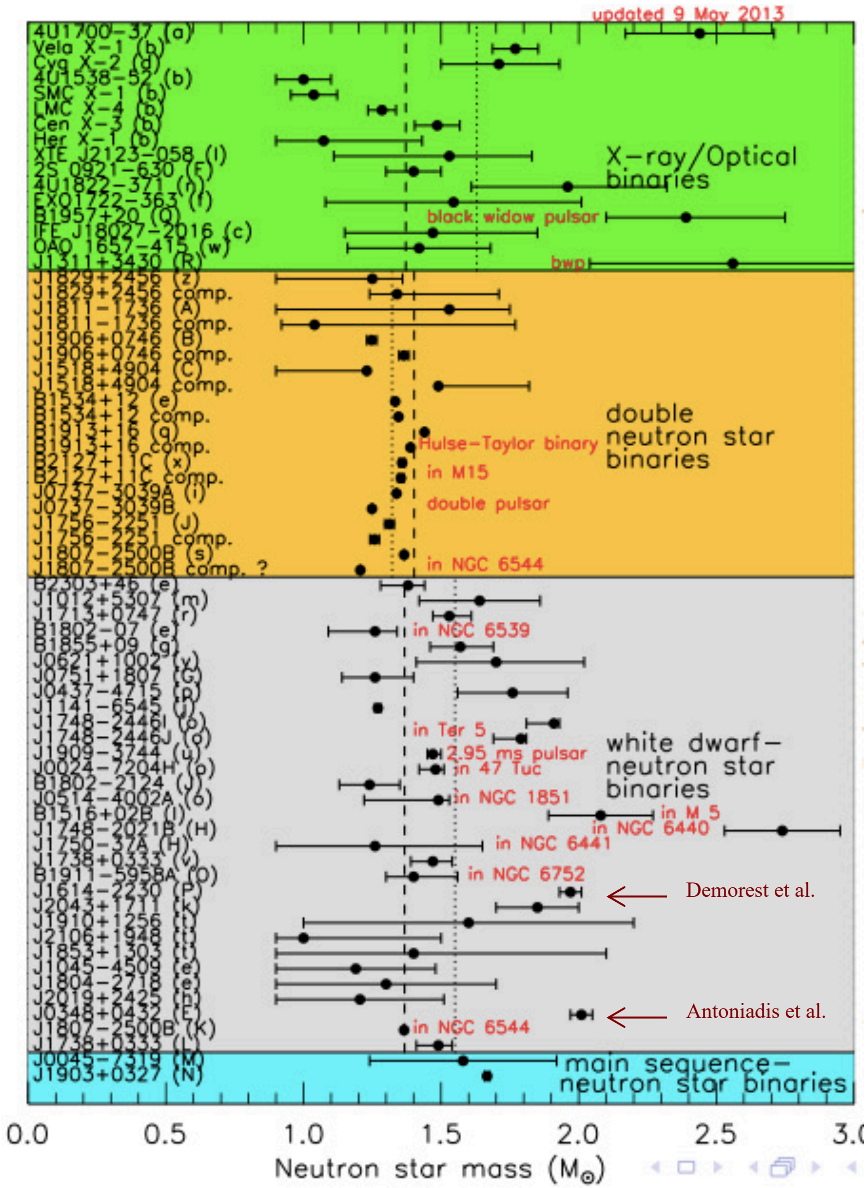

updated from Lattimer 2013

Observation of ~ 2 $M_\odot$ neutron stars imposes a very stringent constraint

Any reliable nuclear EoS should satisfy

$$M_{\max}\left[EoS\right] > 2M_\odot$$

otherwise is rule out

Limits on the Neutron Star Radius

The radius of a neutron star with mass M cannot be arbitrarily small

General Relativity:
a Neutron Star is not a
Black Hole

$$R > \frac{2GM}{c^2}$$

Finite Pressure:
Neutron Star matter cannot
be arbitrarily compressed

$$R > \frac{9}{4}\frac{GM}{c^2}$$

Causality:
speed of sound must
be smaller than c

$$R > 2.9\frac{GM}{c^2}$$

Neutron Star Radii

Radii are very difficult to measure because NS:

- ✧ are very small (~ 10 km)
- ✧ are far from us (e.g., the closest NS, RX J1856.5-3754, is at ~ 400 ly)

A possible way to measure it is to use the thermal emission of low mass X-ray binaries:

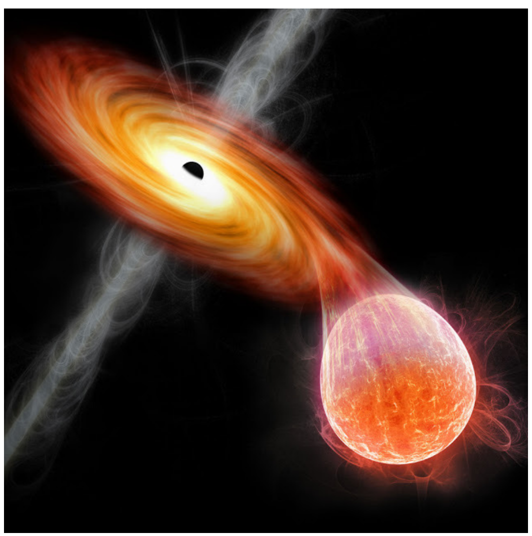

NS radius can be obtained from

✧Flux measurement +Stefan-Boltzmann's law
✧Temperature (Black body fit+atmosphere model)
✧Distance estimation (difficult)
✧Gravitational redshift z (detection of absorption lines)

$$R_\infty = \sqrt{\frac{FD^2}{\sigma_{SB}T^4}} \rightarrow R_{NS} = \frac{R_\infty}{1+z} = R_\infty \sqrt{1 - \frac{2GM}{R_{NS}c^2}}$$

Recent Estimations of Neutron Star Radii

The recent analysis of the thermal spectrum from 5 quiescent LMXB in globular clusters is still controversial

Steiner et al. (2013, 2014)

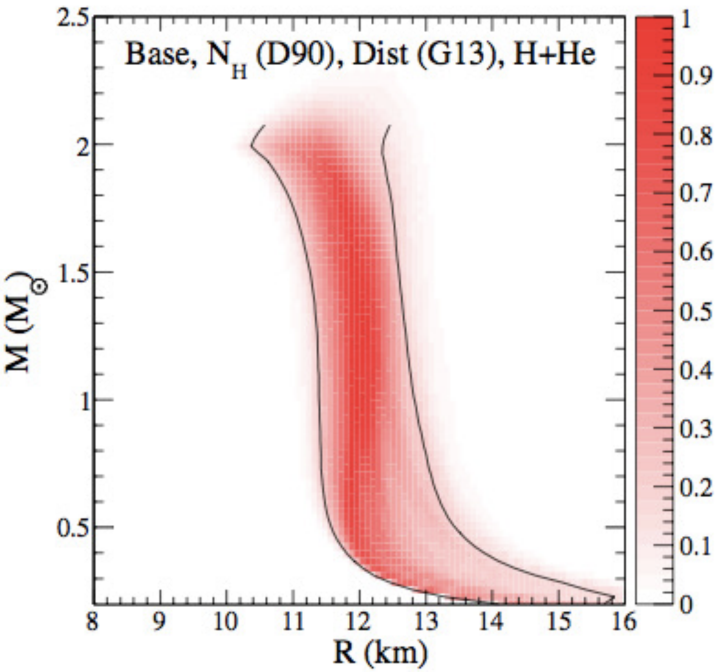

$$R = 12.0 \pm 1.4 km$$

Guillot et al. (2013, 2014)

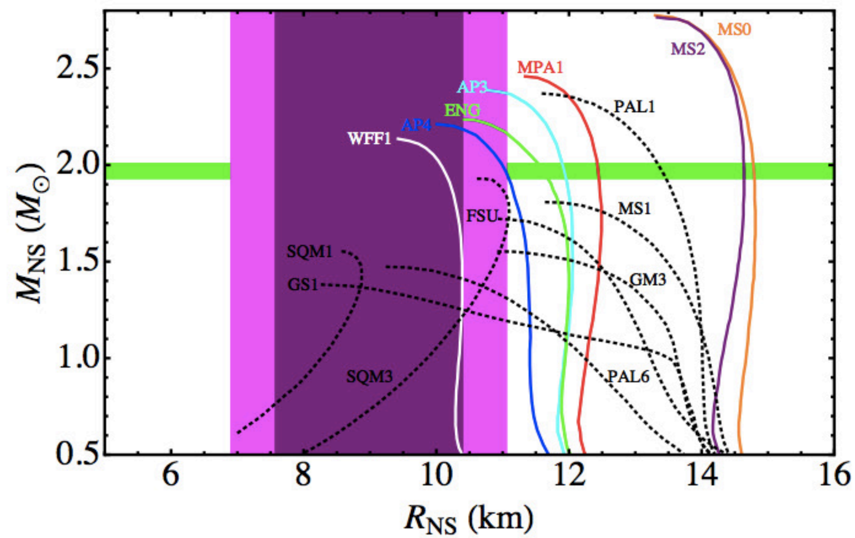

$$R = 9.1^{+1.3}_{-1.5} km$$ 2013 analysis

$$R = 9.4 \pm 1.2 km$$ 2014 analysis

NICER: Neutron Star Interior Composition Explorer

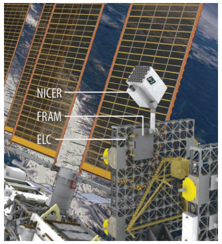

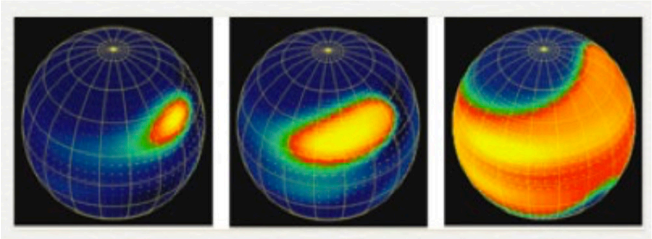

A new way of measuring M & R from rapidly spinning compact stars with a hot spot, based on GR corrections of the signal (M/R) and on Doppler effect (R)

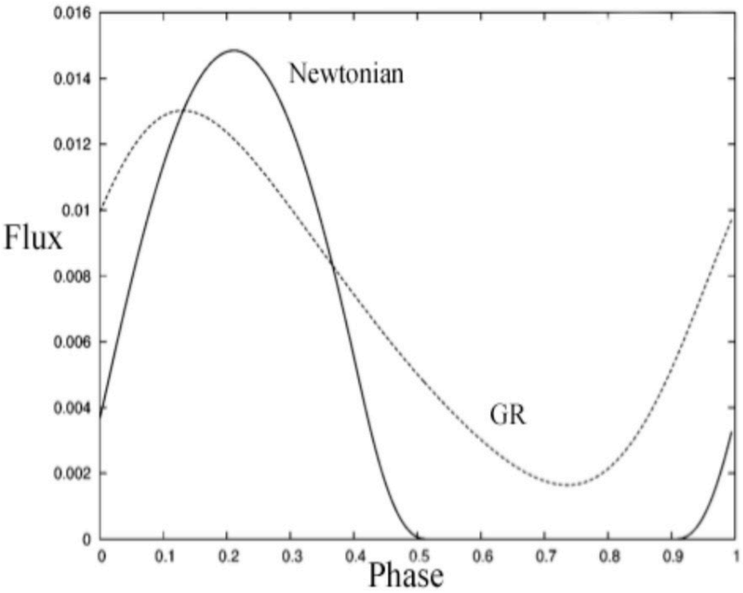

✧ PSR J0740+6620

$$M = 2.072^{+0.067}_{-0.066} M_\odot$$

$$R = 13.7^{+2.6}_{-1.5}\ km$$ Miller et al., arXiv:2105.06979

$$R = 12.39^{+1.30}_{-0.98}\ km$$ Riley et al., arXiv:2105.06980

✧ PSR J0030+0451

$$M/R = 0.156^{+0.008}_{-0.010}$$

$$R = 13.02^{+1.24}_{-1.06}\ km$$ Miller et al., ApJ 887 L24 (2019)

$$R = 12.71^{+1.14}_{-1.19}\ km$$ Riley et al., APJ 887 L21 (2019)

Combined analysis of a few astrophysical data

- NICER PSR J0740+6620 & PSR J0030+0451 (bands)
- GW170817 (from tidal deformability, orange solid/dashed lines)
- RXTE results for the cooling tail spectra of 4U1702-429 (violet line)

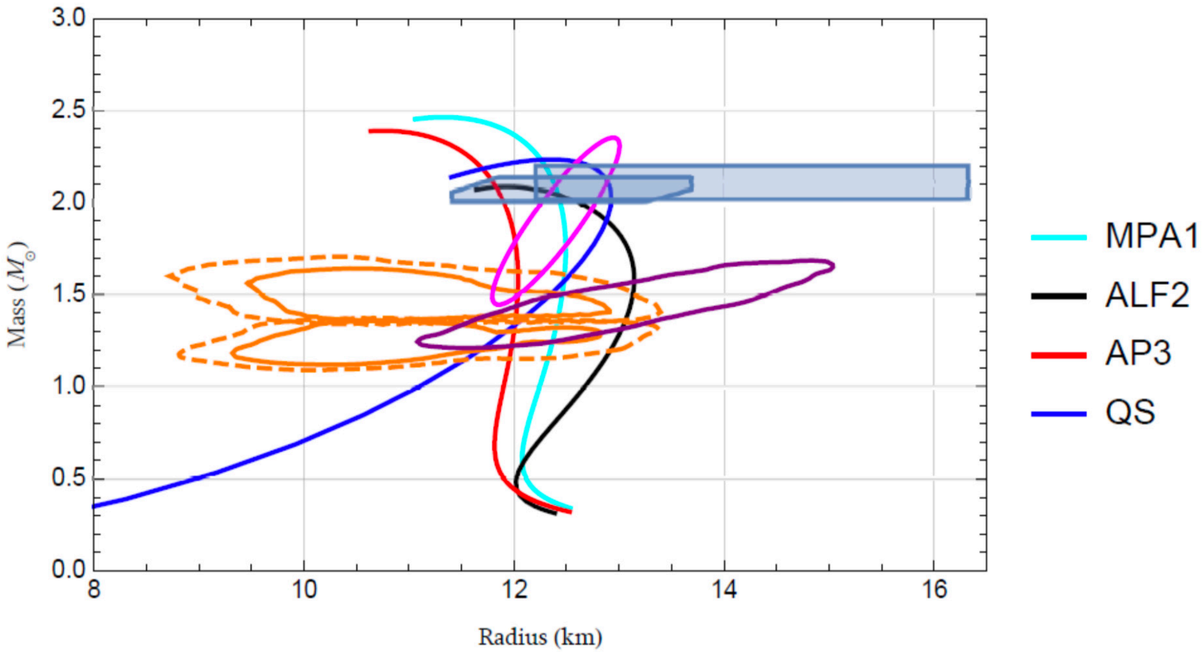

Neutron Star Rotation

Rotation of pulsars can be accurately measured. However, pulsars cannot spin arbitrarily fast. There is an absolute maximum (minimum) rotational frequency (period)

Centrifugal Force = Gravitational Force

⬇

Keplerian Frequency Ω_K
(EoS dependent)

Newtonian Gravity

$$P_{\min} = 2\pi\sqrt{\frac{R^3}{GM}} \approx 0.55\left(\frac{M_{sun}}{M}\right)^{1/2}\left(\frac{R}{10km}\right)^{3/2} \quad ms$$

General Relativity

$$P_{\min} = 0.96\left(\frac{M_{sun}}{M}\right)^{1/2}\left(\frac{R}{10km}\right)^{3/2} \quad ms$$

An observed frequency above the Ω_k predicted by a given EoS would rule out that model

Fasted pulsar known: PSR J1748-2446ad (P=1.39595482 ms)
cannot allow to put stringent constraints on existing EoS

Thermal Evolution of Neutron Stars

Information, complementary to that from mass & radius, can be also obtained from the measurement of the temperature (luminosity) of neutron stars

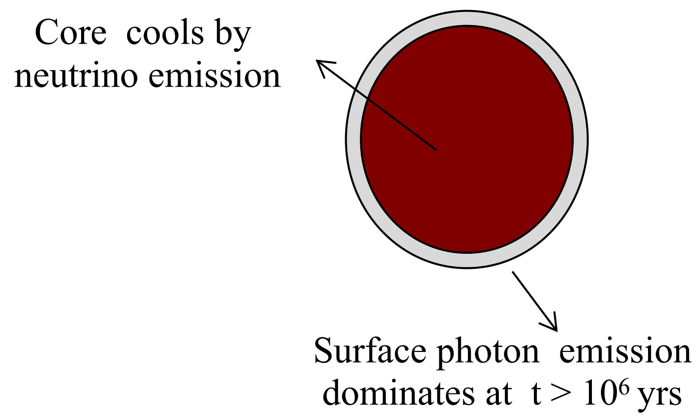

Two cooling regimes

Slow	Fast
Low NS mass	High NS mass

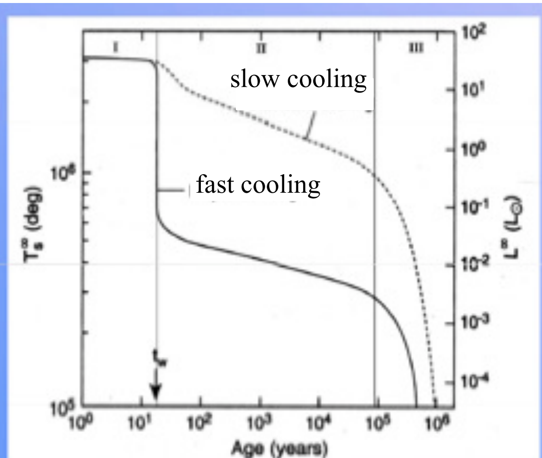

I. Core relaxation epoch

II. Neutrino cooling epoch

III. Photon cooling epoch

$$\frac{dE_{th}}{dt} = C_v \frac{dT}{dt} = -L_\gamma - L_\nu + H$$

✓C_v: specific heat

✓L_γ: photon luminosity

✓L_ν: neutrino luminosity

✓H: “heating”

Strong dependence on the NS composition & EoS

Multi-messenger Observations of the Event GW170817

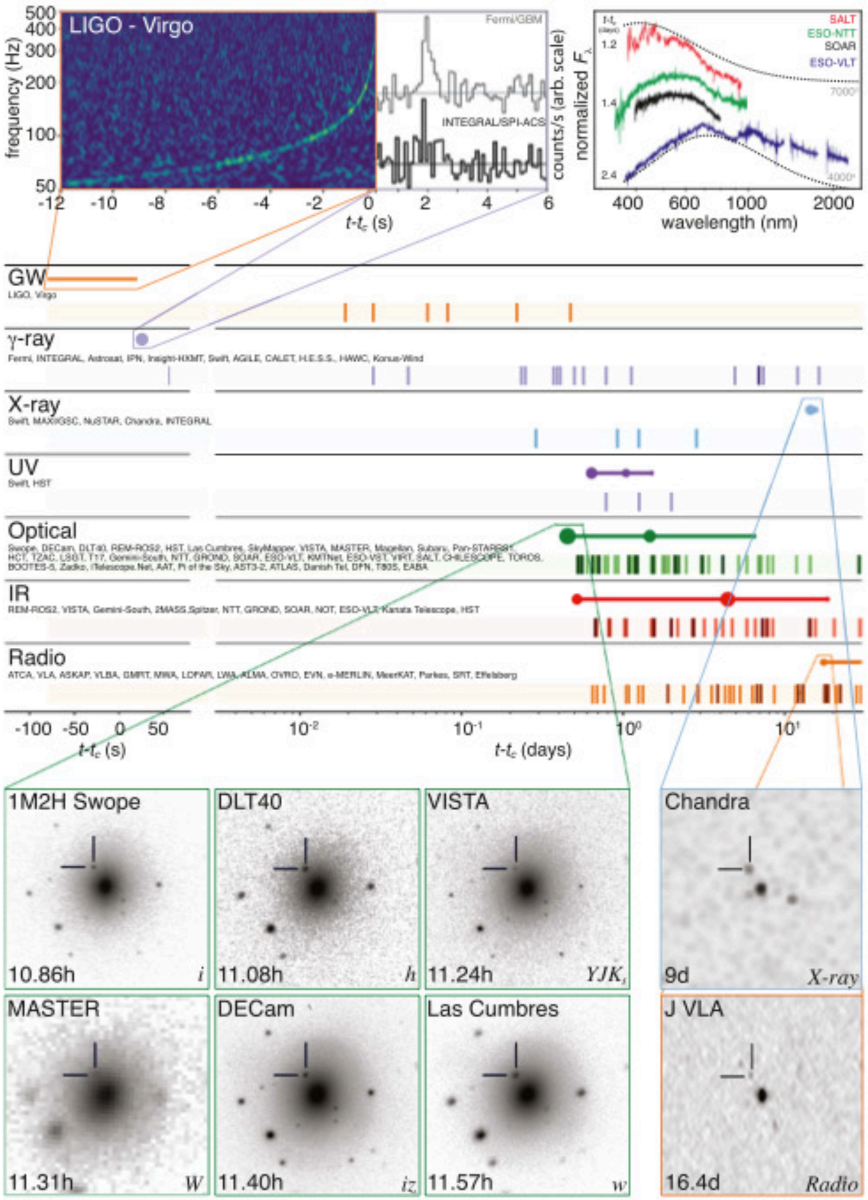

LIGO/VIRGO GW detection with associated electromagnetic events observed by over 70 observatories

- August 17th 2017 12:41:04 UTC

  GW from a BNS merger detected by Adv. LIGO & Adv. VIRGO

- + 1.7 seconds

  GRB (GRB170817A) detected by FERMI γ-ray Burst Monitor & INTEGRAL

- Next hours & days

  - New bright source of optical light (SSS17a) detected in the galaxy NGC 4993 in the Hydra constellation (+10h 52m)
  - Infrared emission observed (+11h 36m)
  - Bright ultraviolet emission detected (+15h)
  - X-ray emission detected (+9d)
  - Radio emission detected (+16d)

First Analysis & Implications of GW170817

The very first analysis of the event GW170817 seem to indicate:

✧ NS radii should be R < 13 km or even smaller than 12 km. Some analysis suggest R < 11 km⟶ **Constraint on the EoS: those predicting large radii excluded ?**

✧ Low value of the upper limit of tidal deformability indicates a **soft EoS**

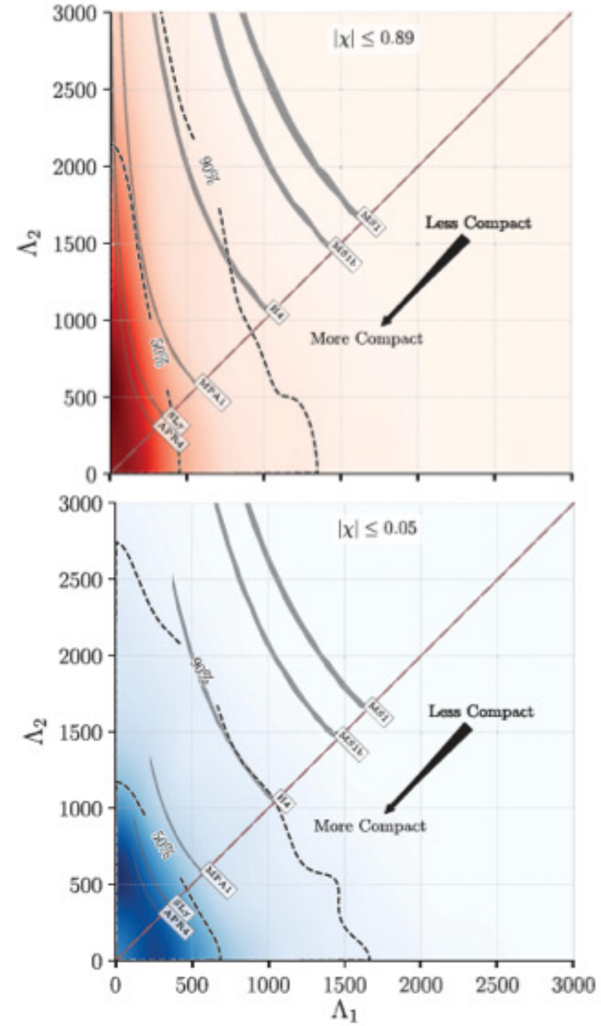

Other neutron star observables

Other NS observables can also help to constraint direct or indirectly the nuclear EoS

✧ Gravitational Redshift:

$$z = \left(1 - \frac{2GM}{c^2 R}\right)^{-1/2} - 1$$

Measurements of z allow to constraint the ratio of M/R

✧ Quasi-periodic Oscillations:

QPO in X-ray binaries measure the difference between the NS rot. freq. & the Keplerian freq. of the innermost stable orbit of matter elements in the accretion disk. Their observation & analysis can put stringent constraints on masses, radii & rotational periods

✧ NS moment of inertia:

$$I = \frac{J(\Omega)}{\Omega}; \quad J(\Omega) = \frac{8\pi}{3}\int_0^R dr r^4 \frac{p(r)+\varepsilon(r)}{\sqrt{1-\frac{2M(r)}{r}}}\left(\Omega - \omega(r)\right)e^{-\nu(r)}$$

Measurements of I could also constraint EoS. But not measured yet. Lower bound can be inferred from timing observations of Crab pulsar

Building the Nuclear EoS

Approaches to the Nuclear EoS: "Story of Two Philosophies"

Ab-initio Approaches

Based on two- & three-nucleon realistic interactions which reproduce scattering data & the deuteron properties. The EoS is obtained by "solving" the complicated many-body problem

- ✧ Variational approaches: FHNC
- ✧ Diagrammatic: methods: BBG (BHF), SCGF
- ✧ Monte-Carlo techniques: VMC, DMC, GMC, AFDMC
- ✧ RG methods: $V_{\text{low k}}$

Phenomenological Approaches

Based on effective density-dependent interactions with parameters adjusted to reproduce nuclear observables & compact star properties.

- ✧ Non-relativistic: Skyrme & Gogny
- ✧ Relativistic: RMF

Non-homogeneous matter

- ✧ SN approximation models: Liquid drop models, TF models, Self-consistent models
- ✧ NSE models: NSE, Virial EoS, models with in-medium mass shifts

Difficulties of ab-initio approaches

- ✧ Different NN potentials in the market … but all are phase-shift equivalent

- ✧ Short range repulsion makes any perturbation expansion in terms of V meaningless. Different ways of treating SRC

- ✧ Complicated channel & operatorial structure (central, spin-spin, spin-isospin, tensor, spin-orbit, …)

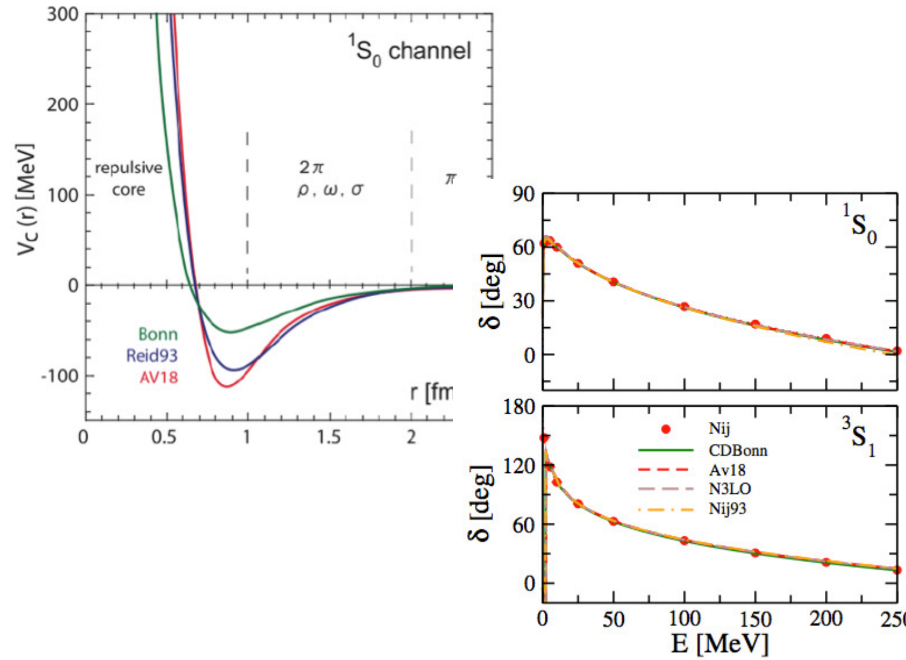

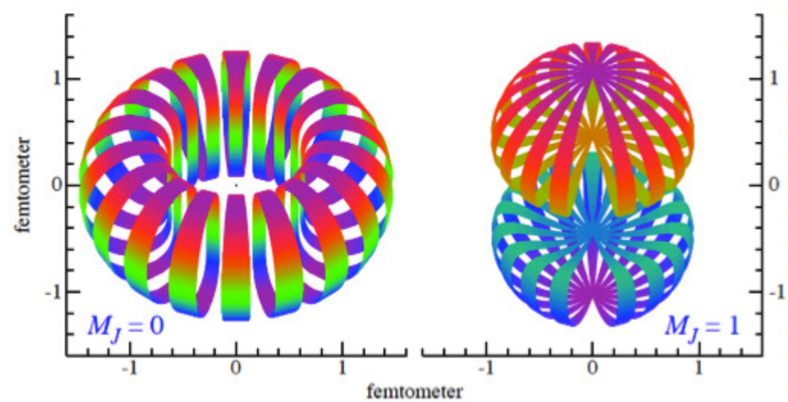

The NN interaction: meson exchange & potential models

✧ Meson Exchange Models:

NN interaction mediated by the exchange of different meson fields (e.g, Bonn, Nijmegen)

- ✧ scalar: σ, δ $\qquad \Gamma_s = 1$
- ✧ pseudocalar: π, K, η $\qquad \Gamma_{ps} = i\gamma^5$
- ✧ vector: ρ, K, ω, ϕ $\qquad \Gamma_v = \gamma^\mu , \quad \Gamma_T = \sigma^{\mu\nu}$

$$L = g_M \Gamma_M \left(\bar{\Psi}_B \Psi_B\right) \phi_M$$

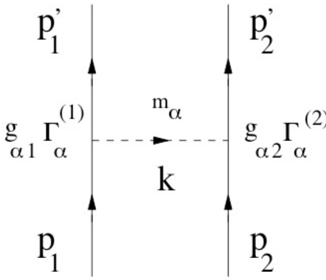

$$\langle p_1' p_2' | V_M | p_1 p_2 \rangle = \bar{u}(p_1') g_M^{(1)} \Gamma_M^{(1)} u(p_1) \frac{P_M}{\left(p_1 - p_1'\right)^2 - m_M^2} \bar{u}(p_2') g_M^{(2)} \Gamma_M^{(2)} u(p_2)$$

Machleidt et al., PR. 149, 1 (1987)
Nagels et al., PRD 17, 768 (1978)

✧ Potential Models:

NN interaction is given by the sum of several local operators (e.g., Urbana, Argonne)

$$V_{ij} = \sum_{p=1,18} V_p(r_{ij}) O_{ij}^p$$

Ex: Local operators of Av18 potential

$$O_{ij}^{p=1,14} = \left[1, (\vec{\sigma}_i \cdot \vec{\sigma}_j), S_{ij}, \vec{L}\cdot\vec{S}, L^2, L^2(\vec{\sigma}_i \cdot \vec{\sigma}_j), (\vec{L}\cdot\vec{S})^2\right] \otimes \left[1, (\vec{\tau}_i \cdot \vec{\tau}_j)\right]$$

$$O_{ij}^{p=15,18} = \left[T_{ij}, (\vec{\sigma}_i \cdot \vec{\sigma}_j) T_{ij}, S_{ij} T_{ij}, (\tau_{zi} + \tau_{zj})\right]$$

Wiringa et al., PRC 51, 38 (1995)

Three-Nucleon Forces

Necessary to:

- ✧ Reproduce the spectra of light nuclei
- ✧ Saturate properly in non-relativistic many-body calculations

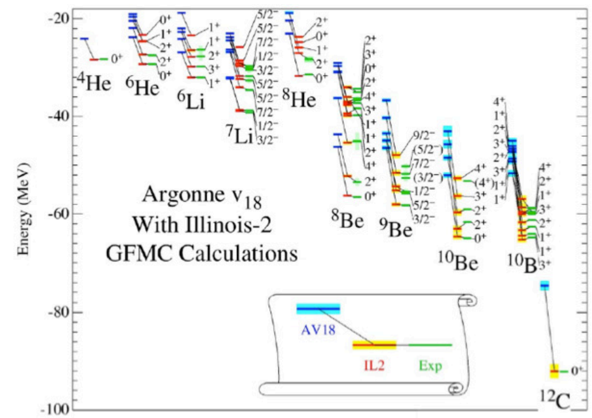

Pieper & Wiringa, ARNPS 51, 53 (2001)

✧ **Urbana-type** $V_{ijk}^{UIX} = V_{ijk}^{2\pi} + V_{ijk}^{R}$

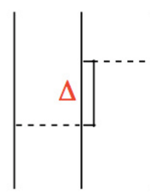

$V_{ijk}^{2\pi}$: Attractive Fujita-Miyazawa force

V_{ijk}^{R} : Repulsive & Phenomenological

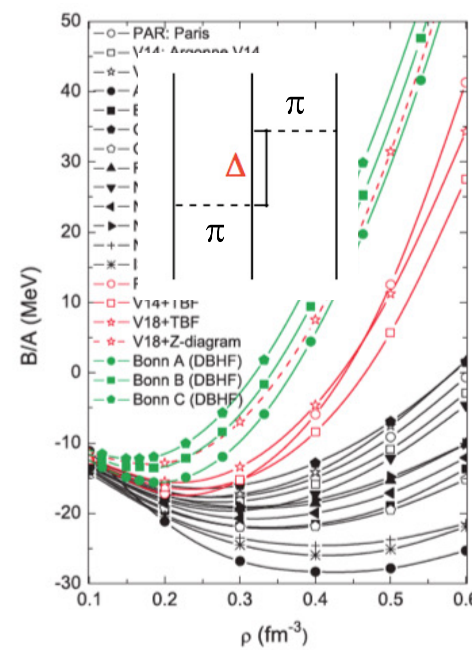

✧ **Microscopic-type**

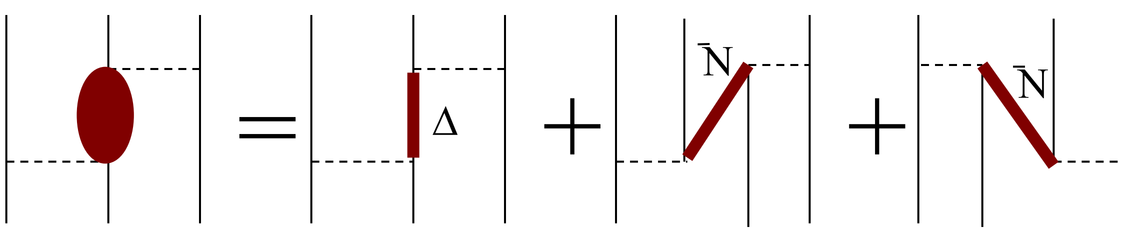

Problem: NNN is not independent of NN

Li et al., PRC 74, 047304 (2006)

The NN interaction: χEFT forces

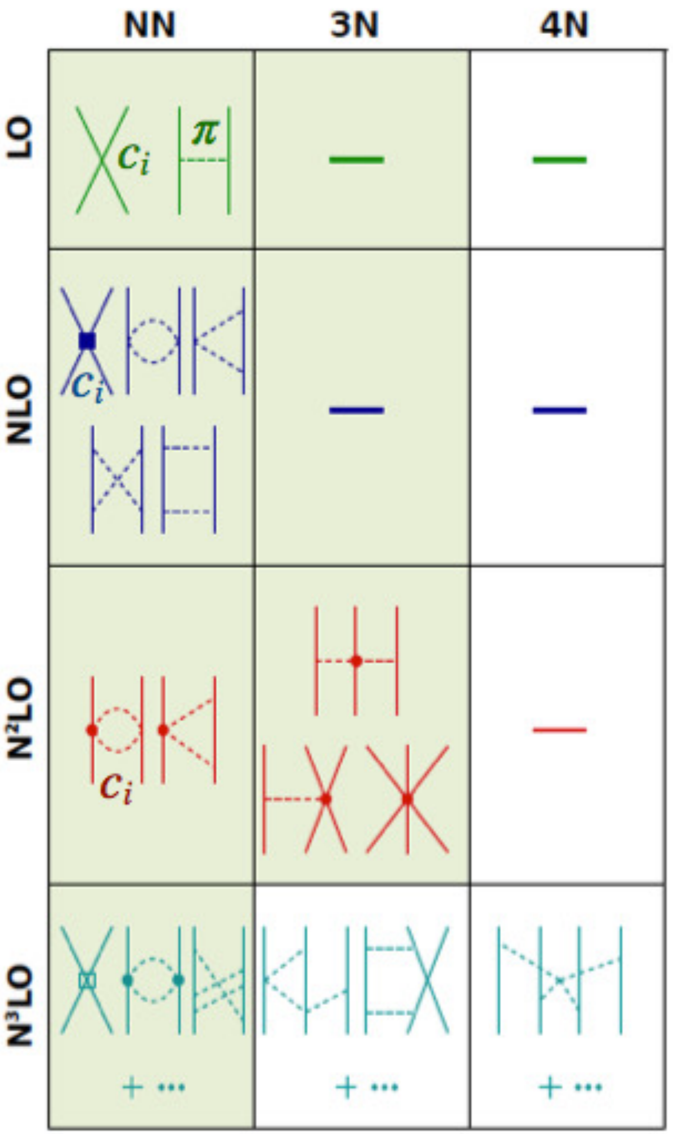

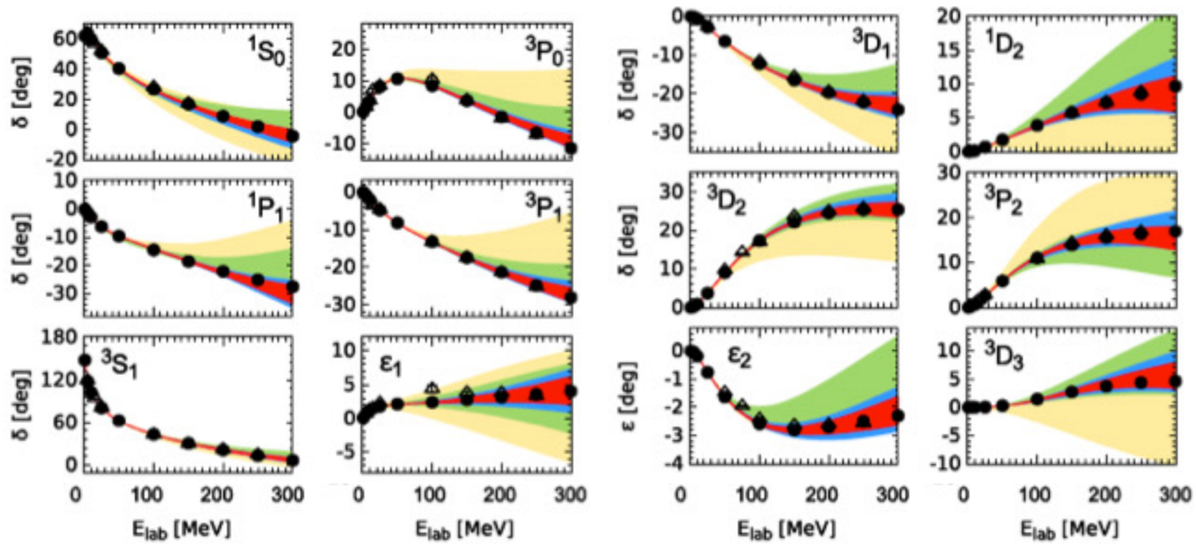

- Starting point: most general effective chiral Lagrangian that respect required QCD symmetries where π & N (recently also Δ) are the relevant d.o.f. of the theory
- Systematic expansion in powers of Q/Λ_χ [$Q=m_\pi$, k; $\Lambda_\chi \sim 1$ GeV]
- Consistent derivation of 2N, 3N, 4N, … forces

Weinberg, PLB 251, 288 (1990); NPB 363, 3 (1991)
Entem & Machleidt, PRC 68, 041001(R) (2003)
Epelbaum et al., NPA 747, 363 (2005)

Variational Approaches

Based on the
variational principle

$$E \leq \min\left\{\frac{\langle\Psi_T|\hat{H}|\Psi_T\rangle}{\langle\Psi_T|\Psi_T\rangle}\right\}, \quad |\Psi_T\rangle = \hat{F}|\Phi\rangle, \quad \hat{F} = \prod_{i>j}\sum_p f^{(p)}(r_{ij})\hat{O}_{ij}^{(p)}$$

correlation operator   uncorrelated w.f.

- ✓ $\Phi(r_1, r_2, \cdots)$: uncorrelated ground-state wave function properly antisymmetrized and product of all possible pairs   of particles (i.e., Slater Determinant)

- ✓ $f(ij)$: correlator factors take into account the correlations of the system. Are determined by means of the Ritz-Raleight variational principle, i.e. by assuming that the mean value of the Hamiltonian reaches a minimum

$$\frac{\delta}{\delta f}\left(\frac{\langle\Psi_T|\hat{H}|\Psi_T\rangle}{(\Psi_T|\Psi_T)}\right) = 0$$

→ The main task of the variational method is to find a suitable ansatz for the correlation factors f. Usually one assumes that $\hat{F}$ can be expanded in the same type of operators of the nucleon-nucleon interaction

$$\hat{F} = \prod_{i<j}\sum_p f^{(p)}(r_{ij})\hat{O}_{ij}^{(p)}$$

Diagrammatic Approaches: BBG theory

Ground state energy of nuclear matter evaluated in terms of the hole-line expansion (perturbative diagrams grouped according to the number of independent hole lines.)

- ✓ Hole-line expansion = expansion in ρ
- ✓ Contribution of diagram with h hole-lines to E/A $\propto \rho^{h-1}$
- ✓ Nuclear matter is a dilute system $c / r_0 < 1$

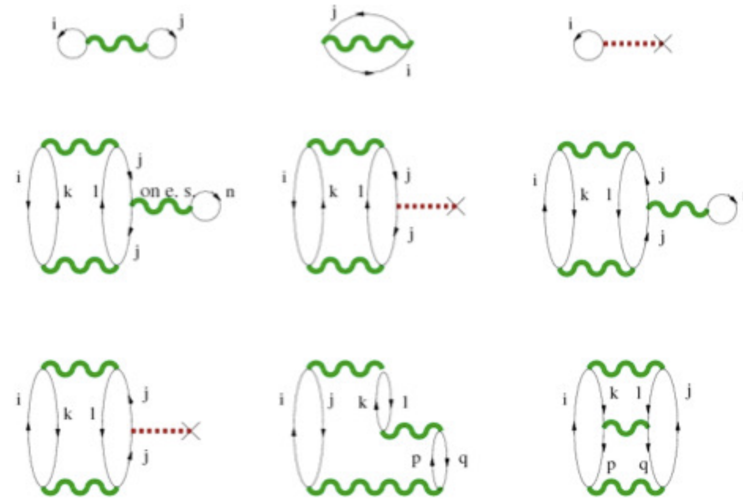

✧ Hole-line expansion derived by means of Brueckner's reaction matrix (G-matrix)

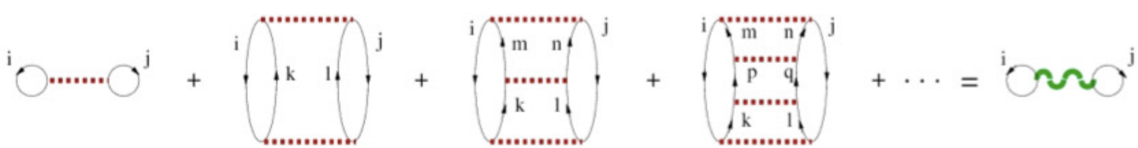

$$G(\omega) = V + V \frac{Q}{\omega - E - E' + i\eta} G(\omega)$$

✧ BHF approximation: leading term of the hole-line

$$E_{BHF} = \sum_{i \le A} \langle \alpha_i | K | \alpha_i \rangle + \frac{1}{2} \mathrm{Re} \left[\sum_{i,j \le A} \langle \alpha_i \alpha_j | G(\omega) | \alpha_i \alpha_j \rangle \right]$$

Infinite sumation of two-hole line diagrams

Day, Rev. Mod. Phys. 39, 719 (1967)

Diagrammatic Approaches: SCGF formalism

Energy obtained from the Galitskii-Migdal-Koltum (GMK) sum rule

$$E=\frac{\nu}{\rho}\int\frac{d^3k}{(2\pi)^3}\int_{-\infty}^{\infty}\frac{d\omega}{2\pi}\frac{1}{2}\left\{\frac{\hbar^2k^2}{2m}+\omega\right\}A\left(\vec{k},\omega\right)f\left(\omega\right)$$

s. p. spectral function FD distribution

✧ Spectral function

$$A(\vec{k},\omega)=\frac{-2\,\mathrm{Im}\,\Sigma(\vec{k},\omega)}{\left[\omega-\frac{\hbar^2k^2}{2m}-\mathrm{Re}\,\Sigma(\vec{k},\omega)\right]^2+\left[\mathrm{Im}\,\Sigma(\vec{k},\omega)\right]^2}$$

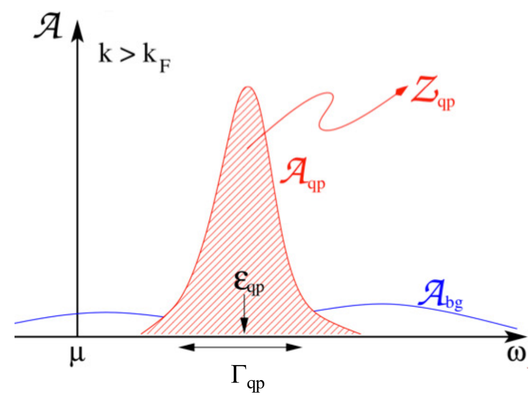

✧ Self-consistent computation scheme

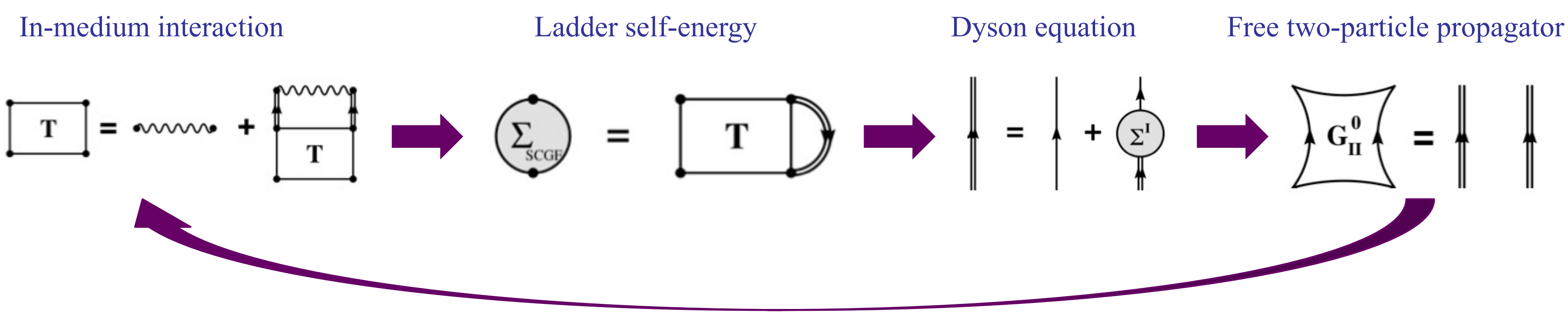

Figures adapted from A. Rios

Carbone et al., PRC 88, 054326 (2013)

Quantum Monte-Carlo Techniques

✧ VMC:

Evaluate energy & other observables using the Metropolis method

$$\langle \hat{O} \rangle = \frac{\sum_i \langle \Psi(\vec{R}_i) | \hat{O} | \Psi(\vec{R}_i) \rangle / W(\vec{R}_i)}{\sum_i \langle \Psi(\vec{R}_i) | \Psi(\vec{R}_i) \rangle / W(\vec{R}_i)}$$

Wiringa et al., PRC 62, 014001 (2000)

✧ DMC:

Model a diffusion process rewriting the Schoedinger equation in imaginary time

$$i\frac{\partial}{\partial t}|\Psi\rangle = \hat{H}|\Psi\rangle \Rightarrow -\frac{\partial}{\partial \tau}|\Psi\rangle = \hat{H}|\Psi\rangle$$

Anderson, J. Chem. Phys. 63, 1499 (19755)

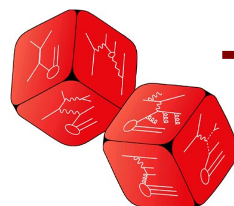

✧ GFMC:

Sample a trial wave function by evaluating path integrals of the form

$$|\Psi(\tau)\rangle = \prod \exp\left[-\left(\hat{H} - E_0\right)\Delta\tau\right]|\Psi_V\rangle$$

$$|\Psi(\tau)\rangle \underset{n\to\infty}{\longrightarrow} |\Psi_0\rangle$$

Carlson et al., PRC 68, 025802 (2003)

✧ AFDMC:

Rewrite Green's function in order to change the quadratic dependence on spin & isospin operators to a linear one by introducing Hubbard-Stratonovich auxiliary fields

Gandolfi et al., PRC 79, 054005 (2009)

Low momentum NN interaction

<u>Idea</u>: start from a realistic NN interaction & integrate out the high momentum components

$\boxed{V_{\text{low k}}}$

- ✓ phase shift equivalent
- ✓ energy independent
- ✓ softer (no hard core)
- ✓ hermitian

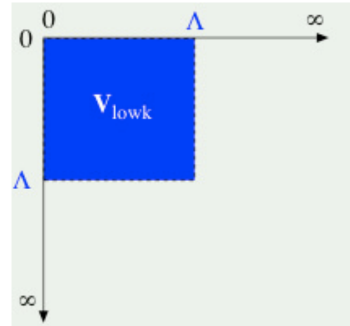

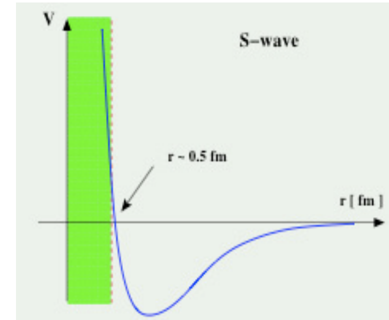

✧ Modified Lippmann-Schwinger Equation

$$T(k',k;E_k) = V_{low\,k}(k',k) + \frac{2}{\pi} P \int_0^{\Lambda} dq q^2 V_{low\,k}(k',q) \frac{1}{E_k - H_0(q)} T(q,k;E_k)$$

demanding $\boxed{\dfrac{dT}{d\Lambda} = 0}$

✧ Renormalization Group Flow Equation

$$\frac{d}{d\Lambda} V_{low\,k}(k',k) = -\frac{2}{\pi} \frac{V_{low\,k}(k',\Lambda) T(\Lambda,k;\Lambda^2)}{E_k - H_0(\Lambda)}$$

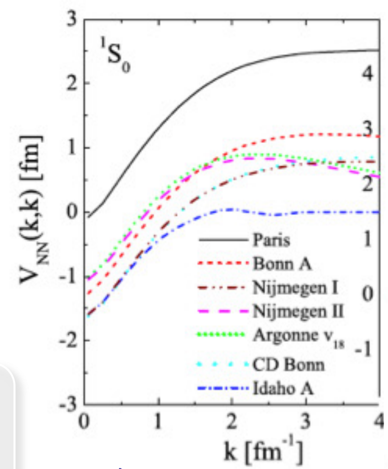

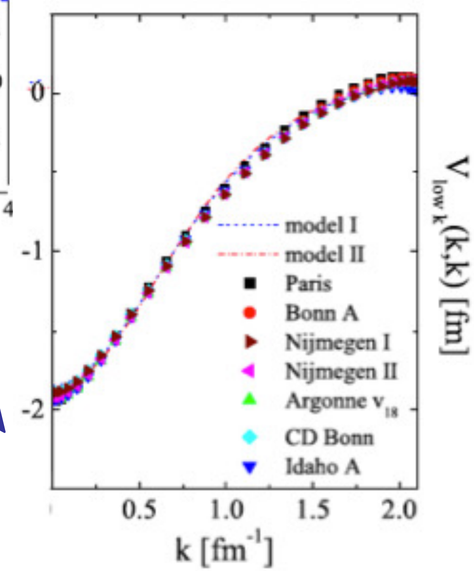

$V_{\text{low k}}$ evolved potentials

Bogner et al., Phys. Rep. 386, 1 (2003)

Phenomenological Models: Skyrme & Gogny interactions

✧ Skyrme interactions:

Effective zero-range density dependent interaction

$$\hat{V}(\vec{r}_1,\vec{r}_2) = t_0\left(1 + x_0\hat{P}_\sigma\right)\delta(\vec{r}_{12}) + \frac{t_1}{2}\left(1 + x_1\hat{P}_\sigma\right)\left[\hat{k}^{'}\delta(\vec{r}_{12}) + \delta(\vec{r}_{12})\hat{k}^{2}\right]$$

$$+t_2\left(1 + x_2\hat{P}_\sigma\right)\hat{k}'\delta(\hat{r}_{12})\hat{k} + \frac{t_3}{6}\left(1 + x_3\hat{P}_\sigma\right)\rho^{\alpha}(\vec{R}_{12})\delta(\hat{r}_{12})$$

$$+iW_0\left(\hat{\sigma}_1 + \hat{\sigma}_2\right)\left[\hat{k}^{'} \times \delta(\hat{r}_{12})\hat{k}\right]$$

Evaluation of the energy density in the HF approximation yields for nuclear matter a simple EDF in fractional powers of the number densities. Many parametrizations exist

Skyrme, Nucl. Phys. 9, 615 (1959)

✧ Gogny interactions:

Effective finite-range density dependent interaction

$$\hat{V}(\vec{r}_1,\vec{r}_2) = \sum_{j=1,2}\exp\left(-\frac{r_{12}^2}{\mu_j^2}\right)\left(W_j + B_j\hat{P}_\sigma - H_j\hat{P}_\tau - M_j\hat{P}_\sigma\hat{P}_\tau\right)$$

$$+t_0\left(1 + x_0\hat{P}_\sigma\right)\rho^{\alpha}(\vec{R}_{12})\delta(\hat{r}_{12})$$

$$+iW_0\left(\hat{\sigma}_1 + \hat{\sigma}_2\right)\left[\hat{k}^{'} \times \delta(\hat{r}_{12})\hat{k}\right]$$

Due to the finite-range terms the evaluation of the energy density is numerically more involved. Less number of parametrizations in the market

Brink & Boeker, NPA 91, 1 (1967)

Phenomenological Models: Relativistic Mean Field Models

Based in effective Lagrangian densities where the interaction is modeled by meson exchanges

$$L = L_{nuc} + L_{mes} + L_{\mathrm{int}} + L_{nl}$$

$$L_{nuc} = \sum_{i=n,p} \bar{\psi}_i \left(\gamma_\mu i\partial^\mu - m_i\right)\psi_i$$

$$L_{mes} = \frac{1}{2}\left(\partial^\mu \sigma \partial_\mu \sigma - m_\sigma^2\right) + \frac{1}{2}\left(\partial^\mu \vec{\delta} \partial_\mu \vec{\delta} - m_\sigma^2\right) - \frac{1}{4} G_{\mu\nu} G^{\mu\nu} + \frac{1}{2} m_\omega^2 \omega_\mu \omega^\mu - \frac{1}{4} H_{\mu\nu} H^{\mu\nu} + \frac{1}{2} m_\omega^2 \vec{\rho}_\mu \cdot \vec{\rho}^\mu$$

$$L_{\mathrm{int}} = -\sum_{i=n,p} \bar{\psi}_i \left[\gamma_\mu \left(g_\omega \omega^\mu + g_\rho \vec{\tau} \cdot \vec{\rho}^\mu\right) + g_\sigma \sigma + g_\delta \vec{\tau} \cdot \vec{\delta}\right]\psi_i$$

$$L_{nl} = -\frac{A}{3}\sigma^3 - \frac{B}{4}\sigma^4 + \frac{C}{4}\left(\omega_\mu \omega^\mu\right)^2 + D\left(\omega_\mu \omega^\mu\right)\left(\vec{\rho}_\mu \cdot \vec{\rho}_\mu\right)$$

Nucleon & meson equations of motion are derived from the Lagrangian density and usually self-consistently solved in the mean field approximation where mesons are treated as classical fields and negative-energy states of nucleons are neglected

Boguta & Bodmer, NPA 292, 413 (1977)

Serot & Walecka, Adv. Nuc. Phys. 16, 1 (1986)

EoS for non-homogeneous nuclear matter

Non-uniform nuclear matter is present in the NS crust and SN cores (low ρ, low T). Till now only two types of phenomenological approaches have been used to describe it:

Single-nucleus approximation models

Composition of matter is assumed to be made of one representative heavy nucleus (the one energetically favored) + light nuclei (α particles) or unbound nucleons

- ✓ (Comprenssible) Liquid-Drop models
- ✓ (Extended) Thomas-Fermi models
- ✓ Self-consistent mean-field models

Nuclear Statistical Equilibrium models

Composition of matter is assumed to be a statistical ensemble of different nuclear species and nucleons in thermodynamical equilibrium

- ✓ (Extended) NSE
- ✓ Virial EoS
- ✓ Models with in-medium mass shifts

The final message of this talk

- Major experimental, observational & theoretical advances on understanding the nuclear EoS have been done in the last decades & will be done in the near future

- The isoscalar part of the nuclear EoS is rather well constrained

- Why the isovector part is less well constrained is still an open question whose answer is probably related to our limited knowledge of the nuclear force and, particularly, of its spin & isospin dependence

- ✧ You for your time & attention
- ✧ The organizers for their invitation